Fabrication and Optical Properties of 2D Photonic Crystal Assisted Thin Film Phosphors

Jeong Rok Oh, Ki-Young Ko, and Young Rag Do
Dept. of Chemistry, Kookmin University, Seoul 136-702, Korea
TEL:82-2-910-4893, e-mail: yrdo@kookmin.ac.kr.

Keywords : thin-film phosphors, photonic crystals, extraction efficiency

Abstract

This presentation introduces a simple strategy for producing 2D photonic crystal layers (PCL) with different structures. In an attempt to improve extraction efficiency from the thin film phosphors (TFPs), this study have examined the effects of the structural variables of the 2D PCLs on the light extraction efficiency of TFPs.

1. Introduction

There have been many studies focusing on overcoming the significant discrepancies between the high internal efficiency and poor external efficiency of film-type emitters, such as thin film phosphors (TFPs).[1,2] These discrepancies are mainly due to the total internal reflection (TIR) at their interfaces, where there are significant differences in refractive index between the luminescent layer and nearby layer/air. By introducing two dimensional (2D) photonic crystal layers (PCLs), the light extraction can be improved significantly by out coupling of the remaining guided modes. Previously, we demonstrated the enhanced extraction emission of guided modes in TFPs by adding 2D PCLs on a TFP.[3-5] In agreement with the results for PC LEDs and PC OLEDs, these improvements in extraction efficiency of TFPs are due to the leaky and/or Bragg scattering produced by the periodic arrays in the 2D PCLs.[6] In this presentation, we discuss the fabrication processes, and the effect of structural variables of 2D PCLs on the extraction efficiency of TFPs to compare the perturbation capability of the light confined inside the high-index phosphor layer.

2. Experimental

The only difference in the fabricating process between the triangular-lattice nanorod and air-hole arrays is the different order of applying the Cr masking and nanosphere PC monolayer coating processes. In order to fabricate the 2D SiN_x air-hole array, either a nanosphere monolayer coating process was carried out in advance or the Cr-mask coating process was performed in advance for the triangular-lattice nanoholes. Here, a 2D triangular-lattice air-hole PCL was fabricated on a $Y_2O_3:Eu^{3+}$ TFP by NSL. PS nanospheres with a diameter of 580nm were distributed carefully over the water surface until its surface was completely covered. The close packing domains of the PS nanosphere monolayers are still small and have some irregular shapes. In order to promote crystal growth of the close packing domain, gentle waves of the water medium were generated by slow and careful agitation of the vessel, which was followed by the addition of a few drops of a 1w/w % of sodium dodecyl sulfate (SDS) solution. The resulting defect-free 2D PCL floating on the water surface was transferred by scooping with a 1x1 cm^2 $Y_2O_3:Eu^{3+}$-coated sapphire substrates with a top SiN_x layer deposited by plasma-enhanced chemical vapor deposition (PECVD). The transferred, well-ordered, PS nanospheres on the substrate in monolayer form were thinned by O_2 plasma to the intended diameter. After this step, the substrate was loaded immediately into a thermal evaporation system and a 23nm-thick Cr metal mask was deposited. The PS spheres used as a mask for physical vapor deposition were removed by dissolution in chloroform with ultra-sonication. Consequently, a Cr mask with triangular lattice photonic crystal patterns was clearly defined throughout the surface of the substrate. They were then transferred into the top SiN_x layer by a CF_4-based RIE followed by the removal of a used Cr metal mask with O_2 and Cl_2 based RIE to form the 2D triangular–lattice air-hole PCLs on the $Y_2O_3:Eu^{3+}$ TFPs.

For fabrication of 2D triangular-lattice nanorod PCL on a $Y_2O_3:Eu^{3+}$ TFP by nanosphere lithography (NSL), $SiN_x/Y_2O_3:Eu^{3+}$-coated sapphire substrate was loaded into a thermal evaporation system for the

deposition of a 23nm-thick Cr metal mask. The defect-free 2D PS nanosphere monolayer floating on the water surface was transferred by scooping it up with a 1x1 cm^2 $Y_2O_3:Eu^{3+}$-coated sapphire substrate, which had been coated with a 23nm-thick Cr film as a hard mask and a SiN_x film, several hundreds of nanometers in thickness, as the high refractive index part of a 2D PCL by thermal evaporation and PECVD, respectively. The transferred, well-ordered, PS nanospheres in monolayer form on the substrate were thinned by O_2 plasma to the intended diameter. PS nanospheres with a tailored diameter were used as an etching mask for the formation of 2D hexagonal lattice Cr dot patterns during the O_2 and Cl_2-based RIE process. The used PS nanospheres were eliminated by dissolving them in chloroform with ultra-sonication. Consequently, the hexagonally arrayed Cr metal dots are clearly defined throughout the surface of the substrate, and transferred to a SiN_x layer by a CF_4-based RIE followed by the removal of the used Cr metal mask with an O_2 and Cl_2 based RIE to form the 2D triangular–lattice nanorod PCLs on $Y_2O_3:Eu^{3+}$ TFPs.

The 2D square-lattice SiN_x nanorod or air-hole PCLs were fabricated using the laser hologram lithography (LIL) pattering and an RIE processes consecutively. The only difference in fabricating the 2D square-lattice SiN_x nanoarrays between the nanorods and air-holes was the use of a negative photoresist (N-PR) or a positive-photoresist as a mask layer for making the Cr nanoarrays. Here, a 2D square-lattice air-hole PCL was fabricated on a $Y_2O_3:Eu^{3+}$ TFP by NSL. First, a 115nm-thick negative photoresist (N-PR) film was spin-coated on a $Y_2O_3:Eu^{3+}$-coated sapphire substrate, which had been coated with a 40nm-thick Cr film, as the hard mask and a SiN_x film, several hundreds of nanometers in thickness, as the high refractive index part of a 2D PCL by thermal evaporation and PECVD, respectively. A N-PR-coated substrate was then baked at 95℃ for 1min for a soft bake. The 2D square lattice holes were patterned in the PR film by exposing a N-PR film to 325nm linearly polarized He-Cd laser with a two-step irradiated LHL, in which after first irradiating a N-PR film from one angle, the substrate was rotated 90° and again irradiated under the same conditions. Subsequently, it was baked at 95℃ for 20 s as a post-exposure bake. A two-dimensionally irradiated N-PR film was developed immediately with tetramethylammonium hydroxide (TMAH) in a constant shaking motion. Consequently, a 2D square lattice hole-patterned PR film was obtained on the surface of the Cr film. The remaining water was removed by a hard bake at 95℃ for 20sec. The PR film with 2D air-hole patterns resulted from hologram lithography was used as a mask to form the Cr hard mask pattern using the Cl_2 and O_2-based RIE process. 2D square lattice hole patterns in the Cr film were then transferred onto a SiN_x film using CF_4-based RIE, and the used Cr metal mask was dry etched to form a transparent SiN_x film on a $Y_2O_3:Eu^{3+}$ film with a 2D air hole pattern.

To Fabricate a 2D square-lattice SiN_x nanorod PCL on a $Y_2O_3:Eu^{3+}$ TFP by LIL, a 120nm-thick positive photoresist (P-PR) film was spin-coated on a $Y_2O_3:Eu^{3+}$-coated sapphire substrate to fabricate 2D air-hole arrays, which had been coated with a 40nm-thick Cr film as a hard mask and a SiN_x film, several hundreds of nanometers in thickness, as a high refractive index part of a 2D PCL by thermal evaporation and PECVD, respectively. The P-PR-coated substrate was baked at 95℃ for 1min for a soft bake. The 2D square lattice PR nanorods were patterned by exposing the P-PR film to a 325nm linearly polarized He-Cd laser using a two-step irradiated LHL, in which after first irradiation of a P-PR film from one angle, the substrate was rotated 90° and again irradiated under the same conditions. The substrate was then baked at 95℃ for 1min as a post-exposure bake. A two-dimensionally irradiated P-PR film was developed immediately with tetramethylammonium hydroxide (TMAH) in a constant shaking motion. Consequently, 2D square lattice PR dot patterns were clearly defined on the surface of the Cr film. In order to evaporate the remaining water, a hard bake was carried out at 95℃ for 1min. This square lattice dot patterned PR film from hologram lithography was used as a mask to form a Cr hard mask pattern using a Cl_2 and O_2-based RIE process. The Cr metal dot patterns were then transferred to a SiN_x film using CF_4-based RIE, and the used Cr metal mask was dry etched to form a transparent 2D SiN_x nanorod PCL on a $Y_2O_3:Eu^{3+}$ film.

To fabricate $Y_2O_3:Eu^{3+}$ films, we used a Pechini type of sol-gel reaction.[7] Yttrium nitrate, europium nitrate, and citric acid were used as precursors in the sol-gel reactions. Stoichiometric amounts of yttrium nitrate and europium nitrate were dissolved in 2-methoxyethanol, and the appropriate amounts of citric acid were added. The ratio of metal cations to citrate anions was 1:2. After complete mixing, a homogeneous, transparent solution was obtained. A 2% formaldehyde solution by volume was added to

the solutions as a drying control chemical additive (DCCA). In the preparation of each coating, a few drops of a semi-gel solution were placed on a 2x2 cm^2 square sapphire substrate (KMT Corporation, (0001) plane, two-side polished) and spun at 2000 rpm for 50 seconds. The substrate was then dried in air at 100°C, and baked at 600°C. Thicker $Y_2O_3:Eu^{3+}$ film phosphors were prepared by repeating the whole process, i.e. increasing the number of coatings. Finally, the $Y_2O_3:Eu^{3+}$ thin-film coated sapphire substrates were annealed at 800°C for 2 hours in air. The dopant concentration was fixed at 9.0 mol% according to the optimum Eu^{3+} concentration.

3. Results and discussion

Fig. 1 shows schematic diagrams of the light path in a conventional thin film phosphor and a thin film phosphor coated with 2D PCL arrays. The modes of emitted light of conventional and 2D PCL-assisted film phosphors can be divided into upward and downward emitted light modes and the guided light modes. A thin film phosphor coated with 2D PCL arrays shows different perturbation capability of upward and downward emitted light modes and the guided light modes with different structures of 2D PCLs. First, we discuss the perturbation capability of different types of 2D PCLs on the extraction efficiency of TFPs.

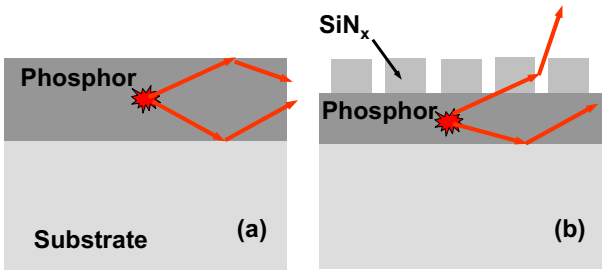

Fig. 1. Schematic diagrams of the light paths in (a) a thin film phosphor on a flat glass substrate, (b) a thin film phosphor coated with a 2D PCL layer.[3]

Although the introduction of a 2D PCL is an effective method for improving the photoluminescence (PL) efficiency of a TFP, the experimentally obtained enhancement of the PL efficiency is still lower than expected.[7] Secondly, we discuss the several reasons for this mismatch between the expected and obtained enhancement of PL efficiencies have been suggested based on recent reports: (i) the difficulties in controlling the structural parameters of the PCLs; (ii) the difference between the crystallinity of the TFPs on flat substrates and those on 2D PCL-assisted substrates; (iii) the intrinsic optical parameters of the TFPs; and (iv) the difference between the thermal expansion coefficients of TFPs and substrates after the annealing process.

Very recently, Ganesh et al. reported significant enhancement in fluorescence from quantum dots on the surface of a 2D PC by engineering the PC to possess leaky eigenmodes at the absorption and emission wavelengths of the quantum dots (QDs).[8] Various TFPs with high PL efficiency is needed to meet the requirements of a variety of applications, such as lighting and flat panel displays. In order to maximize the PL efficiency of various TFPs, it is essential to understand the effect of varying the structural parameters of 2D PCLs on their absorption and extraction efficiency of TFPs. Thirdly, we discuss this improvement in excitation as well as extraction efficiency was attributed to the leaky and/or Bragg scattering produced by the 2D periodic array.

Fig. 2 shows atomic force microscopy (AFM) plan view images of the 2D SiN_x PCLs with triangular-lattice and square-lattice patterns of circular nanorod or air-holes with the same lattice constant and height. Both NSL and LIL were carried out successfully to produce millions of nanorods and nano air-holes with a triangular-lattice and square-lattice. It is evident from these images that a change in structures of 2D nanoarrays can be achieved with good controllability using NSL or LIL.

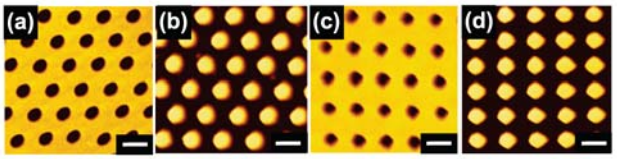

Fig. 2. Top view AFM images of the 2D nanorod and nano air-hole arrays: (a) triangular-lattice air-hole, (b) triangular-lattice nanorod, (d) square-lattice nanorod, (e) square-lattice air-hole PC arrays coated on $Y_2O_3:Eu^{3+}$ TFPs. Scale bars: 500nm.

Fig. 3 (a), (b) show plots of the normally directed PL emission spectra for conventional flat TFPs and for two structures of 2D nanorod or nanohole PC coated TFPs under excitation at 254 nm. The emission

spectra shown in Fig. 3 indicate that almost all the light emission in the 2D nanoarray coated Y_2O_3:Eu^{3+} thin film emanates from the typical $^5D_0 \rightarrow {}^7F_J$ transitions of trivalent europium at the C_2 sites in the cubic structure.

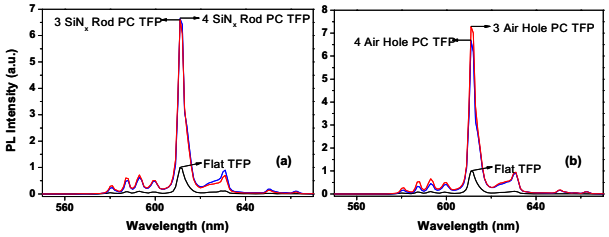

Fig. 3. The relative emission spectra from the normally directed PL measurements under excitation at 254 nm of Y_2O_3:Eu^{3+} TFPs coated with (a) triangular and square–lattice SiN_x nanorod PCLs and a conventional flat thin film, (b) triangular and square–lattice SiN_x air-hole PCLs and a conventional flat thin film.

Both figures suggest that the emission intensity of all types of 2D SiN_x nanorod or nanohole array-coated samples is much higher than that of flat conventional Y_2O_3:Eu^{3+} thin film. The normally directed PL intensity of the nanorod sample was 6.5 and 6.6 times greater for the square-lattice and triangular, respectively, than that of the flat Y_2O_3:Eu^{3+} sample at the same wavelength. Similarly, the normally directed PL intensity of the air-hole sample was improved by factors of 6.7 and 7.3 for the square-lattice and triangular, respectively. Therefore, there is larger improvement in the PL intensity as a result of the introduction of PC scattering layers with index contrast at the interfaces between the air and the Y_2O_3:Eu^{3+} thin films.

4. Summary

These Thin film phosphors have several advantages over screened powder phosphors, including reduced outgassing, superior adhesion, high image resolution, good heat resistance, and long-term stability. However, the luminance levels of thin film phosphors mean that they are not promising candidates for emissive display devices such as field emission displays (FEDs), flat discharge lamps, plasma display panels (PDPs) and phosphor converted light emitting diodes (pc-LEDs), because of their low extraction efficiencies. If the commercial use of thin film phosphors is to be realized, the critical problem of their low extraction efficiency must be overcome. Of various solutions for this problem, it is the very effective way to perturb the wave-guiding effect of the thin film phosphor with a 2D periodic photonic crystal layer. In this presentation, we introduce the structural variables of the 2D SiN_x PCLs on the light extraction efficiency of TFPs, to enhance the extraction efficiency of TFPs.

This work was supported by grant number 2008-03573 of the Nano R&D Program through the Korea Science and Engineering Foundation grant funded by the Ministry of Education, Science and Technology.

5. References

1. S. L. Jones, D. Kumar, K.-G. Cho, R. Singh, and P. H. Holloway, *Displays*, **19**, 151(1999).
2. S. L. Jones, D. Kumar, R. K. Singh, and P. H. Holloway, *Appl. Phys. Lett.*, **71**, 404(1997).
3. Y. K. Lee, J. Y. Cho, C. R. Park, Y.-D. Huh, Y.-C. Kim, and Y. R. Do, *Electrochem. Solid State Lett.*, **10**, H82(2007).
4. K.-S. Sohn, N. Shin, Y.-C. Kim, and Y. R. Do, *Appl. Phys. Lett.*, **85**, 55 (2004).
5. Y. K. Lee, J. R. Oh, Y. R. Do, and Y.-D. Huh, *Appl. Phys. Lett.*, **91**, 231908(2007).
6. S. Fan, P. R. Villeneuve, J. D. Joannopoulos, and E. F. Schubert, *Phys. Rew. Lett.*, **78**, 3294(1997).
7. K.-Y. Ko, Y. K. Lee, Y. R. Do, and Y.-D. Huh, *J. Appl. Phys.*, **102**, 013509(2007).